

# The C49 to C54 Phase Transformation in $\text{TiSi}_2$ Thin Films

R. W. Mann\*

IBM Microelectronics, Essex Junction, Vermont 05452

L. A. Clevenger

IBM T.J. Watson Research Center, Yorktown Heights, New York 10598

## ABSTRACT

The microstructure and kinetics of the polymorphic C49 to C54- $\text{TiSi}_2$  phase transformation have been studied using samples prepared as in self-aligned silicide applications. For C49- $\text{TiSi}_2$  thin films formed at temperatures of 600 and 625°C on (100) single-crystal silicon substrates, the effective activation energy was  $5.6 \pm 0.3$  and  $5.7 \pm 0.08$  eV, respectively, for the C49 to C54 phase transformation carried out in the temperature range 600 to 700°C. We concluded that the transformation process occurred by nucleation and growth of the orthorhombic face-centered (C54) phase from the as-formed orthorhombic base-centered (C49) phase. The Avrami exponent of  $2.2 \pm 0.09$  and the optical observations suggest that most of the nucleation occurred during the beginning of the transformation process.

The C49 to C54 phase transformation in titanium silicide is of significant practical importance in the very large scale integrated (VLSI) industry. Titanium silicide has become the most common silicide in the industry for self-aligned silicide (SALicide) applications because of its combined characteristics of low resistivity, ability to be self-aligned, and relatively good thermal stability.<sup>1-2</sup>  $\text{TiSi}_2$  is a polymorphic material and may exist as an orthorhombic base-centered (C49) phase with 12 atoms per unit cell, or as the thermodynamically favored orthorhombic face-centered (C54) phase with 24 atoms per unit cell.<sup>3</sup> Experimentally, the high resistivity (60 to 90  $\mu\Omega\text{-cm}$ ) metastable C49 phase forms first.<sup>4-5</sup> It is generally accepted that the C49 phase forms first because of a lower surface energy and, hence, barrier to nucleation of this phase.<sup>5-7</sup> The thermodynamic driving force to convert from C49 to C54 is a bulk free-energy difference. The subsequent transformation to the lower resistivity (12 to 20  $\mu\Omega\text{-cm}$ ) C54 phase requires additional thermal energy to overcome the nucleation barrier associated with forming the new surface and the energy required to grow the newly formed crystal.

Surface energy, film thickness, and microstructure are three factors that may influence the phase transformation kinetics. The surface energy can be varied by adding impurities<sup>8</sup> or by varying the substrate materials.<sup>1</sup> The silicide film thickness, which typically decreases with each new technology generation can be varied by changing the formation conditions or the as-deposited thickness.<sup>9</sup> The C49 microstructure can be modulated to some degree by varying the formation temperature.<sup>10</sup> In a previous evaluation using an evaporated film of near stoichiometric (Ti = 1, Si = 2) composition, the effective activation energy for the C49 to C54 transformation was 4.45 eV on an  $\text{SiO}_2$  substrate.<sup>9</sup> In a subsequent study using similar preparation techniques and substrate type, it was shown that the activation energy for this phase transformation may be reduced by adding small quantities [0.3-2.5 atomic percent (a/o)] of antimony.<sup>8</sup>

In VLSI applications, if the transformation is inhibited or fails to occur uniformly, a degradation in circuit performance is observed. In high performance circuits, the resistance-capacitance (RC) delay associated with the lack of phase transformation is typically 5 to 10%, depending on the specific layout used. Figure 1 illustrates the modeled performance impact of the gate conductor sheet resistance for a typical ring oscillator circuit. To minimize this loss in performance, an aggressive thermal treatment is often used to achieve the phase transformation. If the thermal energy used to obtain the phase transformation is excessive, the result is silicide morphological degradation, commonly referred to as agglomeration. Figure 2 summarizes the problem that exists as the VLSI industry continues to scale the line width and film thickness. As illustrated, the problem becomes one of process window narrowing. Some discus-

sion of the narrow linewidth problem has been given previously.<sup>11</sup> Improved understanding and control of the factors governing the phase transformation is essential for extending the use of  $\text{TiSi}_2$  into the near future. Care was taken here to simulate the conditions that are commonly practiced in SALicide applications where it is a generally accepted practice to form the silicide at temperatures between 600 and 700°C, perform a selective etch and then anneal at a temperature >700°C to transform the film to the low resistivity C54 phase.<sup>12,13</sup> Although some discussion has been given earlier to methods for optimizing the nucleation rate during the formation step,<sup>14,15</sup> we focus here on the transformation of films that are essentially devoid of any detectable amount of C54 phase at the outset. The results obtained for samples prepared in this manner differ from those previously discussed.

## Experimental

A 57.5 nm thick film of titanium was evaporated on pre-cleaned (100) silicon wafer substrates that were lightly doped ( $1 \times 10^{15}$  atom/cm<sup>3</sup>) with boron across the thickness of the wafers. Pressure was maintained at  $1 \times 10^{-7}$  Torr during the E-beam evaporation. The samples were sintered in a nitrogen ambient at 600°C for 45 min, or 625°C for 20 min. They were then subjected to a Huang A etch at 65°C to remove the titanium nitride formed at the surface and as much as 10 nm  $\text{TiSi}_2$  that had formed during the sintering process. After the selective etch, a 20 nm plasma-enhanced chemical vapor deposited (PECVD) layer of  $\text{Si}_2\text{N}_4$  was de-

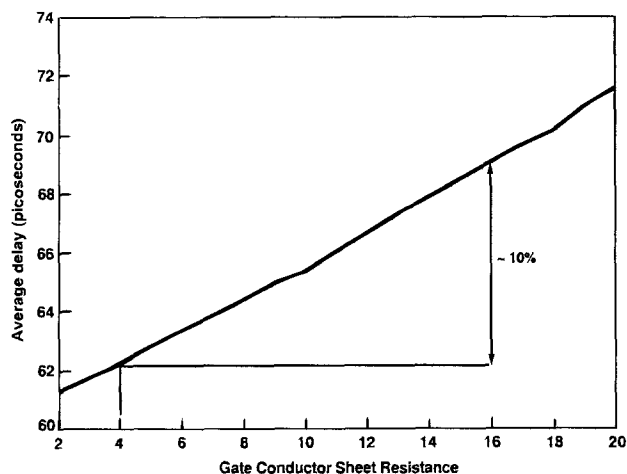


Fig. 1. Ring oscillator stage delay as a function of the gate conductor sheet resistance. A simple complementary metal oxide semiconductor (CMOS) inverter circuit was used in the model. A 10% degradation in performance is predicted if the silicide sheet resistance is  $16 \Omega/\square$  instead of  $4 \Omega/\square$ .

\* Electrochemical Society Active Member.

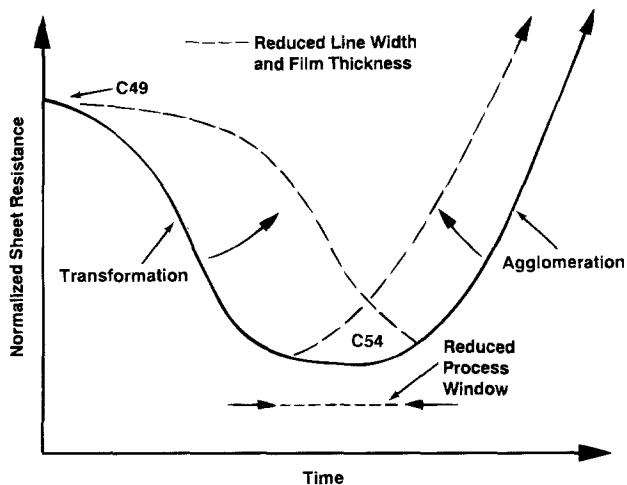


Fig. 2. The process window for obtaining low sheet resistance on narrow lines is shrinking with each technology generation due to reduced linewidths and film thickness.

posited at 400°C to minimize ambient interaction during subsequent anneal steps. This nitride layer was sufficiently thin to allow four-point probe and optical measurements to be made as desired. The samples were then isothermally annealed in the temperature range between 600 and 700°C to accomplish the phase transformation from C49 to C54-TiSi<sub>2</sub>.

The sheet resistance and microstructure of the films were characterized at selected intervals. Rutherford backscattering spectroscopy (RBS) was used to characterize the stoichiometry and thickness after the formation and selective etch steps. A <sup>4</sup>He<sup>+</sup> ion beam with an energy of 1.5 MeV was used to characterize the films. The optical micrographs were obtained using polarized light in a conventional metallurgical microscope.

**Results**

Following the formation and selective etch steps, RBS analysis indicated that the samples formed at 600°C were 25 to 30% thinner than those formed at 625°C and that both sets of films were stoichiometric TiSi<sub>2</sub> (Fig. 3). A small amount of surface oxygen was detected in each sample, which is typical after undergoing the selective etch step. Within the detection limits of the analysis technique (0.1%), no other impurities were found.

At this point the sheet resistance was 11.9 ± 0.4 Ω/□ for the samples formed at 600°C and 9.5 ± 0.2 Ω/□ for those formed at 625°C. The resistivity of the C49-TiSi<sub>2</sub> films prepared as described was ~65 μΩ-cm. The C49-TiSi<sub>2</sub> grain

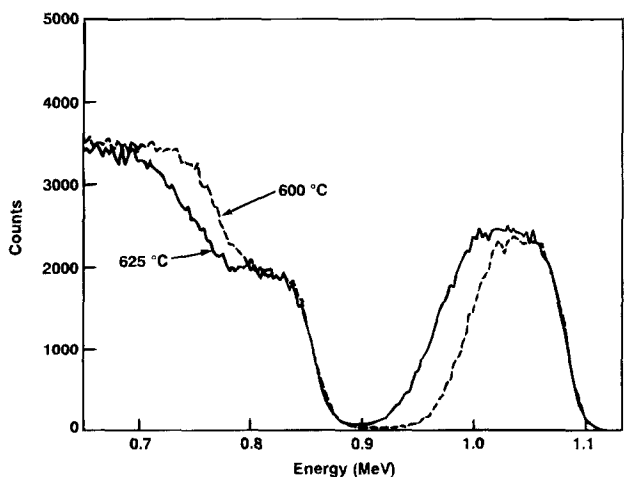


Fig. 3. RBS of the two samples after selective etch. The film composition was stoichiometric TiSi<sub>2</sub> for both samples.

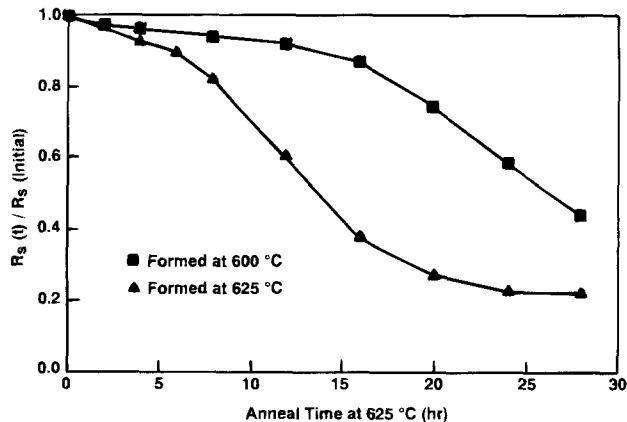


Fig. 4. Normalized sheet resistance as a function of time at temperature for the two sets of samples.

size was below the resolution (0.5-1.0 μm) of the optical technique, regardless of the formation temperature.

The transformation from C49-TiSi<sub>2</sub> to C54-TiSi<sub>2</sub> is accompanied by a corresponding resistivity change. Figure 4 shows the normalized sheet resistance as a function of time at temperature for both sets of formation conditions, 600 and 625°C. Differences in the kinetics can be observed readily between the two samples. To calculate the fraction of the film transformed as a function of time, ζ, we assume a linear relation to the easily measured resistivity.<sup>7,16</sup> The relationship assumed for our calculations is described by

$$\zeta = \frac{\rho_0 - \rho(t)}{\rho_0 - \rho_f} \quad [1]$$

where ρ<sub>0</sub>, ρ<sub>f</sub>, and ρ(t) correspond to the C49-TiSi<sub>2</sub> resistivity, the C54-TiSi<sub>2</sub> resistivity, and the measured resistivity, respectively. After the samples were completely transformed to the final C54-TiSi<sub>2</sub> phase, a resistivity of ~15 μΩ-cm was obtained. Shown in Fig. 5 are the characteristic sigmoidal curves obtained in plotting the fraction of the film trans-

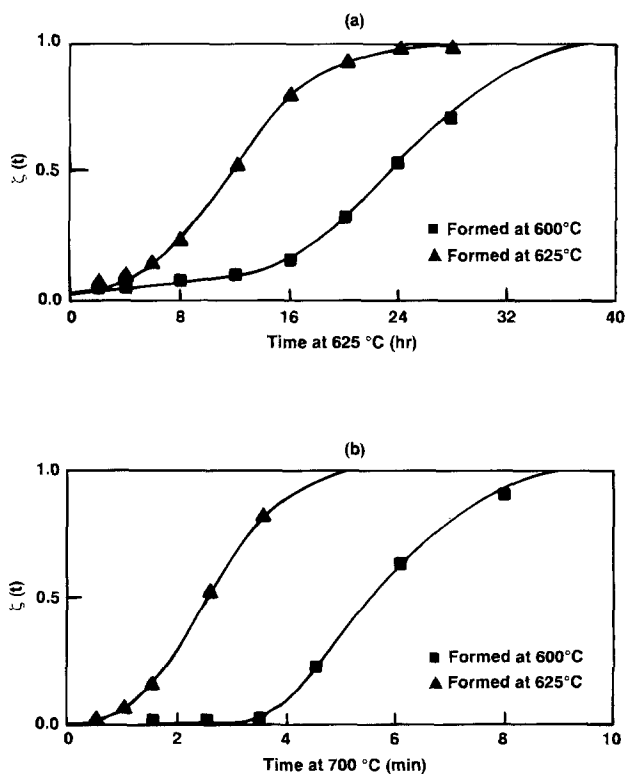


Fig. 5. Fraction of the film transformed to C54 phase TiSi<sub>2</sub> vs. time at 625°C (a) and at 700°C (b).

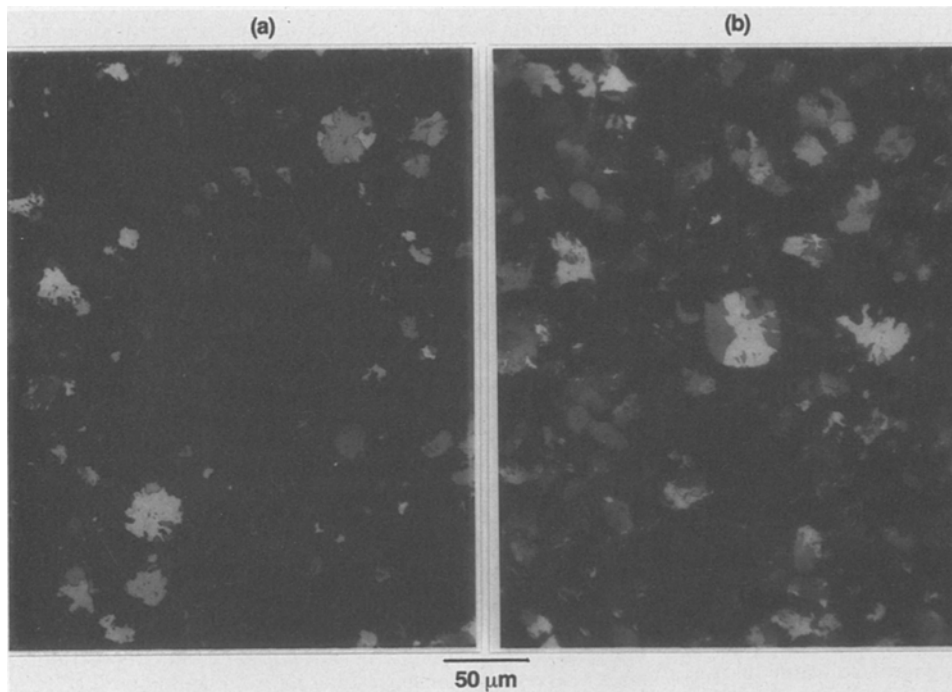


Fig. 6. Optical micrographs showing the radial growth of the C54 phase TiSi<sub>2</sub> crystals. Microstructure after 20 h (a), and 28 h (b), at 625°C. The sample was formed at 600°C.

formed as a function of time at temperature. The curves are indicative of a nucleation and growth mechanism consisting of an incubation or induction period (most pronounced for the samples formed at 600°C), a period of rapid growth, and a final stage of slow completion. Optical micrographs shown in Fig. 6 correspond to the curve in Fig. 5(a) for the sample formed at 600°C and transformed at 625°C. Because the C49-TiSi<sub>2</sub> grains are too small to be distinguished, only the C54-TiSi<sub>2</sub> grains are evident. The two-dimensional grain growth was essentially isotropic, as shown in the micrographs taken after 20 and 28 h at 625°C. After 28 h at 625°C, Fig. 6(b), certain C54-TiSi<sub>2</sub> grains were found with a diameter-to-thickness ratio approaching 1000:1. This is consistent with the thermodynamic barrier to nucleation being higher than the barrier to growth.

The number of optically detectable C54-TiSi<sub>2</sub> grains per unit area increased quickly during the induction period and remained essentially constant for the remainder of the transformation. The C54-TiSi<sub>2</sub> grains then continued to grow until the grain boundaries of adjacent grains met. Approximately  $1 \times 10^{-3}$  grains/ $\mu\text{m}^2$  were observed for the samples formed at 600°C following the induction period of the transformation. The number of grains per square area was 1.5 to 2.5 times higher for the samples formed at 625°C. The optical micrograph data suggest that the bulk of the nucleation occurred primarily at the beginning of the transformation. A crude estimate of the growth rates was obtained by measuring changes in the grain diameter as a function of time. The growth rate observed at 600°C was 0.45  $\mu\text{m}/\text{h}$  and, at 625°C, was slightly less than a factor of two larger (0.8  $\mu\text{m}/\text{h}$ ).

The effective activation energy,  $E_a$ , for the phase transformation was extracted by plotting the natural log of the time at which half the film was transformed vs.  $1/kT$  (Fig. 7). Based on the following Arrhenius relationship, the slope of this plot yields the effective activation energy for the phase transformation

$$\tau_{(\zeta=1/2)} = \tau_0 \exp\left(\frac{E_a}{kT}\right) \quad [2]$$

In this equation,  $\tau_{(\zeta=1/2)}$  refers to the time required to transform half the film to C54 and  $\tau_0$  is a constant with units of time. Although both sets of samples were annealed at 600°C, a lack of sufficient transformation had occurred at 96 h for the C49-TiSi<sub>2</sub> film formed at 600°C to obtain a

value for the fraction transformed,  $\zeta$ , but a small degree of C54 crystal growth was observed in the optical micrographs. This observation was accompanied by a corresponding small change in the sheet resistance for this sample formed and annealed at 600°C.

A suitable representation of the transformation kinetics for the two sets of films is given by:  $\tau_{(\zeta=1/2)} = 5.6 \times 10^{-29} \text{ min} \cdot \exp(5.6/kT)$  for the 53 nm thick TiSi<sub>2</sub> film formed at 600°C; and  $\tau_{(\zeta=1/2)} = 3.7 \times 10^{-30} \text{ min} \cdot \exp(5.7/kT)$  for the 70 nm thick film formed at 625°C.

### Discussion

The shape of the isothermal transformation curves shown in Fig. 5 is characteristic of a nucleation and growth mechanism. For thin films where the growth is essentially two-dimensional, the well-known Johnson-Mehl-Avrami analysis<sup>17</sup> yields

$$-\ln(1 - \zeta) = \pi \delta \int_0^t T^2 N(t - \tau)^2 d\tau \quad [3]$$

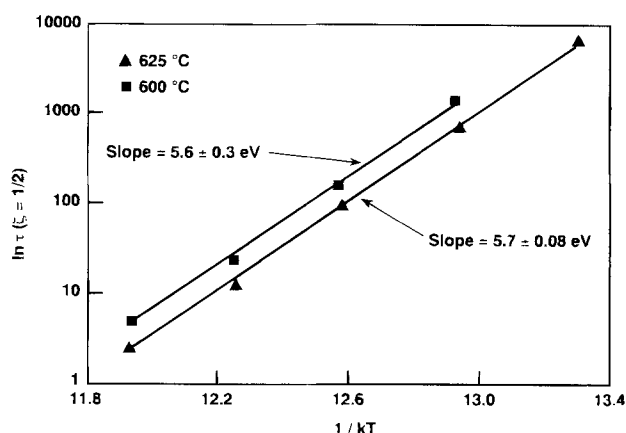


Fig. 7. Arrhenius plots of the time required to transform half the film to C54 TiSi<sub>2</sub> for samples formed at 600 and 625°C. Activation energies for the transformation were  $5.6 \pm 0.3$  eV for the samples formed at 600°C and  $5.7 \pm 0.08$  eV for the samples formed at 625°C.

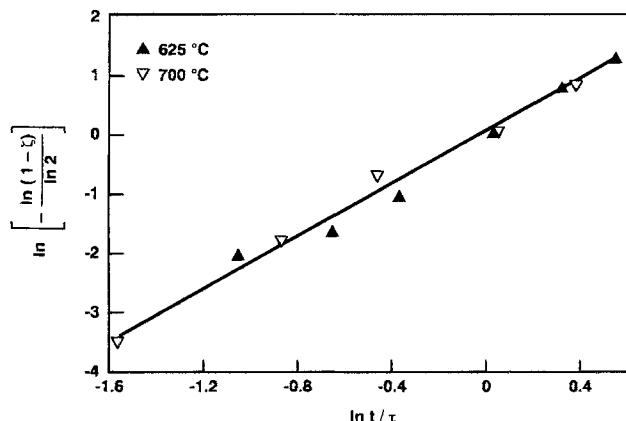


Fig. 8. Log-log plots for determining the mode of transformation for the sample formed at 625°C yielded a value of  $n = 2.2 \pm 0.09$ .

where  $\zeta$  is the fraction transformed,  $\delta$  is the film thickness,  $N$  is the nucleation rate,  $T$  is the growth rate,  $t$  is time, and  $\tau$  is the induction period. Equation 3 can be integrated only by making assumptions about the nucleation and growth rate. Avrami proposed that the general solution to this equation may be expressed as

$$\zeta = 1 - \exp(-Kt^n) \quad [4]$$

where the value  $n$ , referred to as the Avrami exponent, is dependent on the initial boundary condition assumptions for the nucleation and growth. The value for  $K$  is dependent on the initial boundary conditions established by the assumptions for nucleation and growth. For the assumption of constant nucleation rate and isotropic 2D growth for thin films, it can be shown by integration of Eq. 3 that  $n$  is equal to 3 and  $K$  is expressed as

$$K = \frac{(\pi\delta N_0 T_0^2)}{3} \exp\left[-\frac{(E_n + 2E_g)}{kT}\right] \quad [5]$$

Where the nucleation rate is peaked at ( $t = 0$ ),  $n$  becomes equal to 2 and  $K$  is altered accordingly. By taking the log of both sides of Eq. 4 for when  $\zeta = 1/2$ , the result is

$$-\ln\left[\frac{(1-\zeta)}{\ln 2}\right] = \left(\frac{t}{\tau}\right)^n \quad [6]$$

The value of  $n$  can be obtained by taking the log of each side of Eq. 6 where  $n$  becomes the slope

$$\ln\left\{-\ln\left[\frac{(1-\zeta)}{\ln 2}\right]\right\} = n \ln\left(\frac{t}{\tau}\right) \quad [7]$$

A limited investigation of the Avrami exponent was performed for the samples formed at 625°C. As shown in Fig. 8, the slope corresponding to  $n$  was determined to be  $2.2 \pm 0.09$ . This value of  $n$  suggests that the nucleation rate was not constant but was higher during the early stages of the transformation since it is close to the theoretical value of 2 where the nucleation rate is highest at the beginning of the transformation. This is consistent with the C54-TiSi<sub>2</sub> grain count observations made with the optical microscope.

### Conclusion

The transformation kinetics of C49 to C54 titanium silicide have been investigated using conditions similar to

those used in practical applications; namely, salicide practices. We find that for films prepared as in salicide applications, the activation energy is higher than previously quoted values that were prepared differently and were carried out on different types of substrates. The effective activation energy for the C49 to C54 phase transformation was in the range of 5.6 to 5.7 eV when films are formed in a manner simulating the SALicide process. The differences in transformation kinetics between the two sets of samples studied were either due to the film thickness or perhaps differences in the as-formed C49 microstructure. Although only blanket films were studied here, a similar activation energy is expected on patterned narrow lines of C49-TiSi<sub>2</sub> that are devoid of pre-existing C54-TiSi<sub>2</sub> grains. Although this condition may be minimized with higher initial formation temperatures it is not likely to be eliminated completely by purely thermal means. The transformation mode, as determined by the Avrami method where  $n = 2.2 \pm 0.09$ , in conjunction with the optical microscopy data suggests that the nucleation rate was highest near the beginning of the transformation process.

### Acknowledgment

The authors thank Ed Adams for performing the RBS analysis, John Bertsch for his assistance in circuit modeling, Joe Wallace and Dick Courchaine for film depositions, and Francois d'Heurle for his helpful discussions.

Manuscript submitted June 26, 1993; revised manuscript received Dec. 21, 1993.

The IBM Corporation assisted in meeting the publication costs of this article.

### REFERENCES

1. S. P. Murarka, *Silicides for VLSI Applications*, Academic Press, Inc., Orlando, FL (1983).
2. T. Yoshida, S. Ogawa, S. Okuda, T. Kouzaki, and K. Tsukamoto, *This Journal*, **137**, 1914 (1990).
3. F. Laves and H. J. Wallbaum, *Z. Kristallogr.*, **101**, 78 (1939).
4. R. Beyers and R. Sinclair, *J. Appl. Phys.*, **57**, 5240 (1985).
5. P. G. Cotter, J. A. Kohn, and R. A. Potter, *J. Am. Ceram. Soc.*, **39**, 11 (1956).
6. H. Jeon and R. J. Nemanich, *Thin Solid Films*, **184**, 357 (1990).
7. R. D. Thompson, H. Takai, P. A. Psaras, and K. N. Tu, *J. Appl. Phys.*, **61**, 540 (1987).
8. X.-H. Li, R. A. Carlsson, S. F. Gong, and H. T. G. Hentzell, *ibid.*, **72**, 514, (1992).
9. H. J. W. van Houtum and I. J. M. M. Raaijmakers, *J. Mat. Res. Soc. Symp. Proc.*, **54**, 37 (1986).
10. H. J. W. van Houtum, I. J. M. M. Raaijmakers, and T. J. M. Menting, *J. Appl. Phys.*, **61**, 3116 (1987).
11. J. B. Lasky, J. S. Nakos, O. J. Cain, and P. J. Geiss, *IEEE Trans. Electron Devices*, **38**, 262 (1991).
12. D. Pramanik, M. Deal, A. N. Saxena, and O. K. Wu, *Semiconductor Int.*, 94 (May 1985).
13. M. E. Alperin, T. C. Hollaway, R. A. Haken, C. C. Gosmeyer, R. V. Kamvaugh, and W. D. Parmantie, *IEEE Trans. Electron. Devices*, **ED-32**, 141 (1985).
14. R. W. Mann, C. A. Racine, and R. S. Bass, *Mat. Res. Soc. Symp. Proc.*, **224**, 115 (1991).
15. R. W. Mann and C. A. Racine, Abstract 272, p. 438, The Electrochemical Society Extended Abstracts, Vol. 92-1, St. Louis, MO, May 17-22, 1992.
16. R. D. Thompson, J. Angileillo, and K. N. Tu, *Thin Solid Films*, **188**, 259 (1990).
17. J. W. Christian, *Theory of Transformations in Metals and Alloys*, 2nd ed., Part I, Pergamon Press, Oxford (1981).